The *parthenocarpic fruit* (*pat)* mutant of tomato (*Lycopersicon esculentum* Mill.) sets seedless fruits and has aberrant anther and ovule development

Andrea Mazzucato[1],*, Anna Rita Taddei[2] and Gian Piero Soressi[1]

[1]Dipartimento di Agrobiologia e Agrochimica and [2]Centro Interdipartimentale di Microscopia Elettronica, Università degli Studi della Tuscia, Via S. C. de Lellis 1, 01100 Viterbo, Italy

*Author for correspondence (e-mail: soressi@unitus.it)

SUMMARY

Among the different sources of genetic parthenocarpy described in tomato, the mutation referred to as *parthenocarpic fruit* (*pat*) is of particular interest because of its strong expressivity and because it confers earlier ripening, higher fruit set and enhanced fruit quality. As a pleiotropic effect, *pat* flowers have aberrantly developing androecia and reduced male and female fertility. In this work we extend the early description of the *pat* phenotype by investigating the expression of parthenocarpy in three different environments and by using light and scanning electron microscopy to analyse the development of male and female floral organs. The degree of parthenocarpy was high in the three experimental environments and was characterised by a precocious initiation of ovary growth to pre-anthesis floral stages. Aberrations in anther development were evident at flower bud stages and resulted in shorter, irregular and teratoid organs. Ectopic production of carpel-like structures bearing external ovules was evident in the most severely altered androecia. Analysis of ovule development revealed that a fraction of *pat* ovules becomes aberrant from very early stages, having defective integument growth. Meiosis was irregular in aberrant ovules and megaspore or gamete production was severely hampered. The described *pat* syndrome suggests that parthenocarpy in this mutant could be a secondary effect of a gene controlling, at early stages, organ identity and development.

Key words: Female sterility, Homeotic genes, Ovule development, *parthenocarpic fruit*, Tomato

INTRODUCTION

It is well established that fruit set and development is triggered, after pollination and fertilisation, by the coordinated action of growth hormones provided and/or regulated by the pollen grains, the pollen tubes and, ultimately, the developing seeds (Nitsch, 1970; Gillaspy et al., 1993). As an alternative pathway of fruit production, parthenocarpy entails ovary development into a fruit without fertilisation and seed formation, under the guidance of exogenous hormone treatments or endogenous, genetic stimuli. The expression of genetic parthenocarpy is correlated with the accumulation of auxins and gibberellins in the ovaries, which is autonomous and precocious compared to the respective wild-types (George et al., 1984). In consequence, genes for parthenocarpy are thought to affect the pattern of hormone production, transport and/or metabolism, and to overcome a growth substances concentration threshold during the critical period of anthesis, to promote ovary growth in such a way that pollination and fertilisation are no longer needed or possible (Nitsch, 1970).

Parthenocarpy has been extensively studied in tomato because of its application in unfavourable environmental conditions that reduce pollen production, anther dehiscence and, as a consequence, fruit set. Such conditions are normally present in South European Countries when tomatoes are grown in winter in unheated greenhouses or tunnels. Parthenocarpy in tomato can be induced by exogenous hormone treatments (mainly auxins), as established by the pioneering experiments of Gustafson (1936). More recently, different tomato lines carrying gene(s) for parthenocarpy have been discovered or selected (reviewed by Philouze, 1983; George et al., 1984). The *sha* mutant obtained by mutagenesis with ethyl methanesulfonate (EMS) is characterised by a high tendency to parthenocarpy and abnormalities which concurrently affect anther development (Bianchi and Soressi, 1969). The mutant phenotype was first ascribed to the action of two tightly linked genes, *sha* for '*short anthers*' and *pat* for '*parthenocarpic fruit*' (Soressi and Salamini, 1975). The discovery of a spontaneous *sha-pat* mutation in the line 'Montfavet 191' (Pecaut and Philouze, 1978) proved that the described phenotype was caused by a single recessive mutation with pleiotropic effects and the gene was finally named *pat* (Philouze and Pecaut, 1986). The expression of parthenocarpy in *pat* plants is based on an enhanced ovary growth rate during the first 10 days after anthesis, which correlates with a precocious onset of cell divisions in the pericarp and higher auxin, gibberellin and DNA contents in ovaries (Mapelli et al., 1978). Mapelli and coworkers found that ovary weight and the number of pericarp cell layers are higher in *pat* ovaries than in the wild type at anthesis, but did not investigate earlier stages. At maturity

parthenocarpic *pat* fruits are typically about two-thirds of normal size (Bianchi and Soressi, 1969; Falavigna et al., 1978), probably due to decreased cell enlargement, rather than to a lower number of cell layers (Mapelli et al., 1978). Although parthenocarpy expression can be affected by environmental conditions and genetic background (Bianchi and Soressi, 1969), *pat* plants are generally less facultative than lines carrying other genes for parthenocarpy (Philouze and Pecaut, 1986).

In addition to parthenocarpy, the *pat* gene causes aberrations that affect male floral organs. The androecium of *pat* flowers is typically formed by short, irregular and apparently unfused anthers that leave the stigma exerted; dehiscence is preferentially external and although the pollen is fertile, the number of grains is reduced (Bianchi and Soressi, 1969; Philouze and Pecaut, 1986). Moreover, while other sources of genetic parthenocarpy are usually facultative and produce a normal or near normal number of seeds under favourable conditions (Philouze, 1985), female fertility is greatly reduced in *pat*. Apart from a single report of fairly normal seed set under hand pollination (Mapelli et al., 1979), in *pat* genotypes (Bianchi and Soressi, 1969; Falavigna and Soressi, 1987), as well as in the 'Montfavet 191' *pat* allele (Philouze, 1985; Philouze and Pecaut, 1986), the average number of seeds in seeded fruits is always very low. Although embryological investigations were never carried out, it is conceivable that parthenocarpy is accompanied by a large degree of female sterility in this mutant.

Notwithstanding the difficulty of producing seed and the drawback of the smaller fruit size, due to the flower structure which favours cross pollination (Bianchi and Soressi, 1969), the generally improved earliness and higher fruit set (Falavigna and Soressi, 1987), and the improved fruit quality (Falavigna et al., 1978) make this mutant of considerable practical interest.

This paper extends the early description of the *pat* phenotype by investigating the expression of parthenocarpy under different growth conditions with reference to a more complete developmental ladder, spanning stages from young flower bud to mature fruit. The development of male and female floral organs was studied by light (LM) and scanning electron (SEM) microscopy in both wild-type and mutant plants.

MATERIALS AND METHODS

Plant material

Seeds of *Lycopersicon esculentum* Mill. cv. Chico III (hereafter referred to as wild-type, WT) and the corresponding near-isogenic parthenocarpic *pat* line (hereafter referred to as *pat*) were sown in Jiffy pots containing loam-sand-peat (1:1:2). At the five leaf stage, some of the plantlets were pricked out into 25 cm plastic pots and thereafter fertilised weekly with a commercial fertiliser (21N-7P-14K plus oligoelements). At the appearance of the first floral cluster, potted plants were transferred to one of two growth chambers illuminated for 16 hours a day with fluorescent tubes at approximately 125 µE m^{-2} sec^{-1}. Plants were submitted to a high temperature regime (HTR) of 26±1°C during the day and 18±1°C during the night in one chamber and to a low temperature regime (LTR, 22±1°C day, 10±1°C night) in the other. Six plants per line (divided into two replicates) were placed in each chamber. In spring 1996, 16 plantlets per line (divided in two replicates) were directly pricked out in a tunnel at Viterbo (42°26'N, 12°04'E), Italy, under a natural temperature regime (NTR). The mean maximum temperature was 29.3°C and the mean minimum temperature 12.2°C, while the mean natural photoperiod was 14.5 hours. Plants were grown under normal cultural practices in all three environments.

Flowers and berries were sampled throughout the experiments, examining the second to the fourth cluster in WT and *pat* plants, according to nine developmental classes. The developmental classes, designated stages 0 to 8, spanned the steps from young flower bud to mature fruit (Fig. 1A). Stage 0 (flower bud 3.0 to 5.9 mm long) was chosen as the starting point for the investigation, because it is reached 10-15 days before anthesis, a period when parthenocarpy gene expression is sensitive to and stimulated by low night temperatures (George et al., 1984). Because the maximum length of the flower bud is about 12 mm in this lines, stage 0 can be considered a quarter to a half of the maximum; stage 1, half to three-quarters and stage 2, three-quarters to the maximum. In this way, the adopted classification can be applied to different tomato genotypes, whose absolute flower bud dimensions greatly vary.

Expression of parthenocarpy

At least six flowers or berries were sampled at stages 1 to 8 from plants grown in each environment, and per line, stage and replicate. Mean diameter was calculated on dissected ovaries or fruits after measurement of polar and equatorial diameters (±3%). Ovaries at stages 1-5 were measured under a stereo microscope. Differences among mean values were estimated according to the General Linear Model (GLM) for combined experiments (McIntosh, 1983). The variable 'mean diameter' was transformed to a logarithm to meet the assumption of normality of residuals and to improve the readability of time-course histograms. Seeds were extracted at maturity (stage 8), counted and the berries classified as seedless (no seeds), low-seeded (1-5 seeds), medium-seeded (6-30 seeds) and normal-seeded (more than 30 seeds).

Light microscopy

Complete flower buds (stage 0), dissected anthers (stages 1 and 2) and pistils (stages 1-7) of WT and *pat* plants from the HTR and NTR environments were fixed in Karnovsky (2.5% glutaraldehyde, 2% formaldehyde in 0.1 M sodium phosphate buffer, pH 7.2) for 5 hours, dehydrated in a graded ethanol series, and embedded in Technovit 7100 (Heraeus Kulzer) according to the manufacturer's instructions. 5 µm thick sections were cut with a rotatory microtome, stained with 0.1% toluidine blue in 2.5% sodium carbonate buffer, pH 11.0 and mounted with Eukit (Kindler). Callose deposition was investigated in meiotic ovules, both on whole and sectioned specimens, after staining with 0.005% aniline blue in 0.15 M sodium phosphate buffer, pH 9.5, for 20 minutes. LM observations under bright-field and UV light were made using a photo microscope (Microphot FX, Nikon) equipped with an epifluorescence illuminator (DM-455 dichroic mirror, EX-435/10 excitation filter, BA-460 barrier filter) and micrographs taken using Kodak Royal Gold 100 colour films. The number of pericarp cell layers was counted on sectioned ovaries (stages 0 to 6) and the thickness of the pericarp measured (stages 0 to 7). Polar and equatorial diameters were measured and the mean placenta (stages 0 to 6) and ovule or seed (stages 0 to 8) diameter calculated. All microscopic measurements were made with an ocular micrometer. Seed diameters were measured at stage 8 under a stereo microscope. A minimum of six measurements for each feature per genotype and stage of development were made. Average values for ovule or seed diameter were transformed to a logarithm to improve the readability of time-course histograms.

Scanning electron microscopy

Complete flowers (stages 0 to 5) were sampled from the LTR and NTR environments, fixed in 3.0% glutaraldehyde in 0.1 M cacodilate buffer, pH 7.2, for 3 hours, rinsed overnight in cacodilate buffer, post-fixed in 1.0% osmium tetroxide for 10 hours, rinsed again and dehydrated in a graded ethanol series. Specimens were prepared by removing sepals and petals and, in part of them, dissecting individual anthers from the androecium. Ovules were exposed removing part of the pericarp with needles. The material was dried by the critical point method using

Table 1. Patterns of fruit and seed production by wild-type and *pat* plants under different temperature regimes

Environment*	Genotype	No. of plants grown	No. of fruits sampled	Percentage of fruits with seeds in the classes:				Mean number of seeds per fruit†
				0	1-5	6-30	>30	
HTR	WT	6	10	–	–	20	80	42.3
	pat	6	22	59	36	5	–	6.1
LTR	WT	6	10	–	–	10	90	60.7
	pat	6	22	77	23	–	–	1.8
NTR	WT	16	57	–	7	37	56	38.3
	pat	16	66	95	5	–	–	1.3

*Temperature regimes: HRT, high; LTR, low; NTR, natural. See text for details
†Calculated only for fruits with seeds

liquid CO_2 in a Balzers CPD 020 apparatus, attached to specimen holders, and coated with gold in a Balzers Union MED 010 evaporator. Observations were made with a 5200 Jeol JSM scanning electron microscope and photographs taken with TMAX 100 Kodak films.

RESULTS

Expression of parthenocarpy (ovary development)

56-90% of fruits produced by the WT line in the three environments were normal-seeded (Table 1). All the WT fruits from the HTR and LTR regimens had more than 5 seeds, while a small percentage of low-seeded fruits were also produced in the NTR environment. In *pat* plants, the degree of parthenocarpy, detected as percentage of seedless fruits at maturity, ranged from 59 to 95%. On average, WT fruits contained more than 30 seeds in all the environments, while seeded *pat* fruits yielded less than two seeds in LTR and NTR and about six in HTR (Table 1).

Parthenocarpy expression led to different ovary growth patterns in WT (Fig. 1A) and pat (Fig. 1B) plants. From stage 3 onwards the staminal cone of *pat* flowers was crushed by the enlarging ovary, while the WT ovary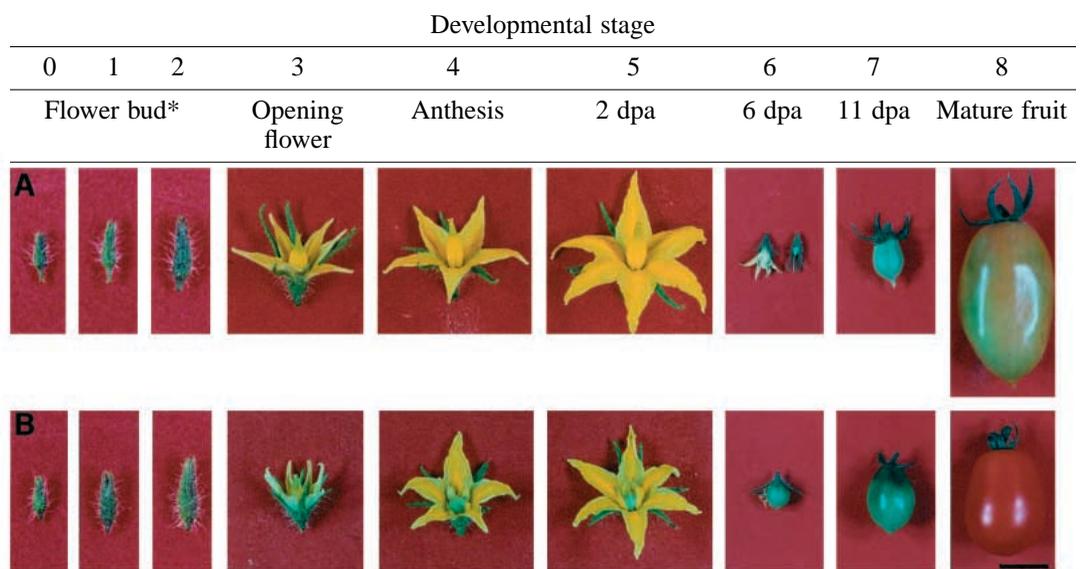 did not increase in size till stage 5 (Fig. 2). As Statistical analysis revealed significant stage/environment and stage/genotype interactions, the GLM procedure was carried out independently for each stage (data not shown). Mean ovary diameter was not significantly different in WT and *pat* flowers at stages 1 and 2, was consistently higher in *pat* from stage 3-7, and higher in fruits from WT plants at stage 8 (Fig. 2).

The number of pericarp cell layers in WT ovaries ranged from 8 to 12 throughout the course of megasporogenesis and megagametogenesis (stages 1-4) and mitotic activity was triggered only

after stage 5, i.e. after fertilisation had taken place: whereas, in *pat* ovaries, it started to increase between stage 2 and 3 (Fig. 3A). Pericarp thickness increase, due to both cell division and elongation, started after stage 5 in WT but was earlier in *pat* ovaries, beginning at stage 4 (Fig. 3B). At anthesis, the pericarp of *pat* ovaries was already structured into a mitotic and a differentiated region and composed on average of 15 cell layers. Placenta development mimicked the pattern of pericarp thickness increase, starting 2 days post anthesis in the WT and at anthesis in *pat* (Fig. 3C).

The androecium of wild-type and *pat* flowers

The androecium of WT flowers was well differentiated and developed by stage 0; there were 5-6 unfused, glabrous anthers (Fig. 4A), which were tetrasporangiate with two lobes and regularly spaced from each other along the lateral surface, where the line of cells between two adjacent locules forms the stomium and permit dehiscence at anthesis (Fig. 4B). Hair initiation was barely evident at stage 0 and was specifically restricted to the lateral and adaxial surfaces of the anther lobes (Fig. 4B, arrows). Androecia from *pat* plants had abnormal anther number and morphology by stage 0 (Fig. 4C). Anthers were distorted and

					Developmental stage				
0	1	2	3	4	5	6	7	8
Flower bud*			Opening flower	Anthesis	2 dpa	6 dpa	11 dpa	Mature fruit

*class limits for flower bud length are 3.0 to 5.9 mm for stage 0, 6.0 to 8.9 for stage 1 and 9.0 to 12 mm for stage 2.

Fig. 1. Developmental stages of tomato flowers and fruits in (A) wild-type and (B) *pat* plants. dpa, days post anthesis. Scale bar, 8 mm for stages 0-2; 10 mm for stages 3-5 and 25 mm for stages 6-8.
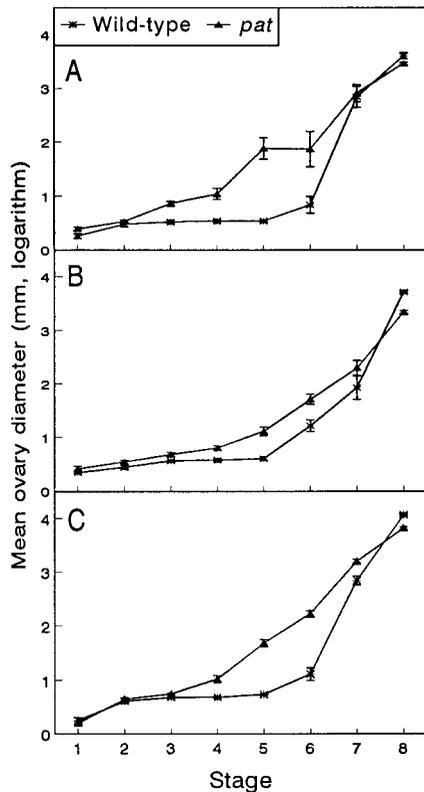
Fig. 2. Dynamics of ovary growth in wild-type (-✳-) and *pat* (-▲-) tomato flowers. Mean ovary diameter under (A) HTR, (B) LTR and (C) NTR growth conditions. Error bars represent s.e.m.

Fig. 3. Dynamics of pericarp and placenta growth in wild-type (-✳-) and *pat* (-▲-) tomato ovaries. (A) Number of pericarp cell layers, (B) pericarp thickness and (C) mean placenta diameter. Error bars represent s.e.m.

locules irregularly orientated, the dehiscence line was often pushed out towards the corolla (Fig. 4D). Although the degree and severity of anther aberrations varied considerably, both within the same flower and among flowers of the same cluster or plant, at least one abnormal anther was found in each investigated *pat* flower. Compared to the WT (Fig. 5A,B), *pat* anthers were often shorter and had distorted lobes (Fig. 5C). Some anthers were abnormally curved (Fig. 5D) with complex structures developing on the adaxial surface (Fig. 5D,E). More careful observation revealed that these structures were carpelloid (Fig. 5F), frequently exhibiting a stigma-like surface (Fig. 5G, arrow and insert) and a placenta-like region bearing external ovules (Fig. 5H,I, arrows). The development of carpelloid structures caused severe distortion of locules, especially on the median-proximal part of the anther, while the distal part developed more or less normally (Fig. 5E,I). The normal adaxial surface pattern of the anther was altered on carpelloid structures which were completely devoided of hairs (Fig. 5I). Despite the presence of differentiating megasporocyte-like cells in some anther-borne ovules, meiotic figures or signs of embryo sac development were never observed.

Microsporogenesis had already occurred in WT stamens by stage 0, when tetrads were present in the locules and the tapetum was still intact (Fig. 6A). Uninucleate pollen grains were released from tetrads by stage 1 (Fig. 6B). On highly abnormal locules of *pat* stamens, meiosis was disturbed and pollen production was hampered by complete degeneration of the sporogenous tissue, which correlated with hypertrophy of
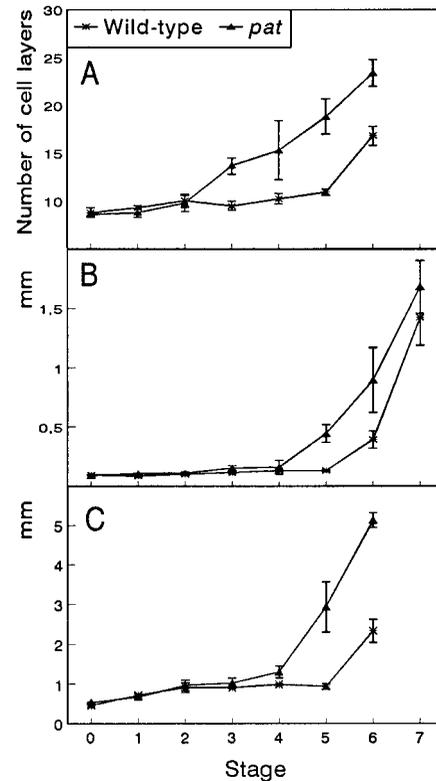
the tapetum (Fig. 6C). In less severely disturbed locules, meiosis appeared to proceed normally and uninucleate pollen was present by stage 1 (Fig. 6D).

The ovule of wild-type and *pat* flowers

WT ovules grew to a diameter of about 180 μm by stage 1 and remained constant in size till stage 5 (Fig. 7A). After this stage, by which time fertilisation is reported to occur in tomato (Rick, 1980), a fraction of the ovules increased dramatically in size, while others developed more slowly or not at all (Fig. 7A). The proportion of undeveloped ovules ranged from 15 to 80% in WT ovaries, apparently regardless of growth conditions (data not shown). Normal ovules in *pat* ovaries followed a similar trend, but their mean diameter was smaller than WT ovules at stages 1 and 2 (Fig. 7B). The few ovules that developed further started to increase in diameter after stage 4. At later stages (7 and 8), seeds were smaller in *pat* than in the WT. The majority of normal *pat* ovules remained undeveloped and failed to increase in size after anthesis (Fig. 7B).

Stage 0 WT ovules were erect and arranged compactly on the placenta surface, the integument was differentiated and partially enveloped the nucellus (Fig. 8A). By stage 1, the asymmetrical growth of the integument covered the nucellus, formed the micropylar opening and bent the ovule towards the placenta in an anatropous position (Fig. 8B). There were few changes in the external structure and size of ovules from stages 2-4 (Fig. 8C). As in WT, *pat* ovules developed normally during stage 0 (Fig. 8D), but alterations began to appear in some of them from
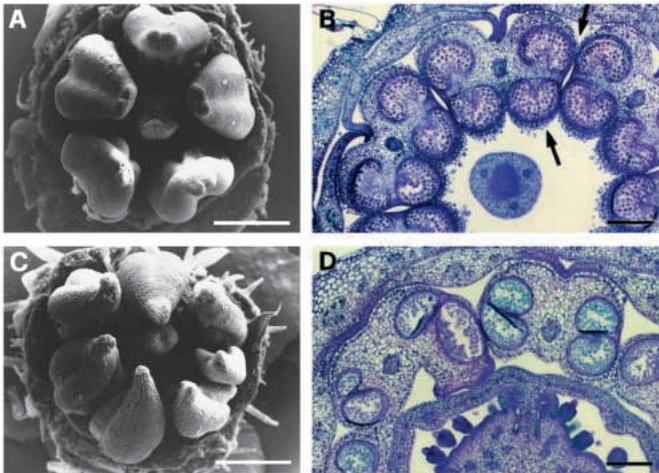
Fig. 4. Androecium morphology of wild-type and *pat* flowers at stage 0 (sepals and petals removed). (A) SEM image and (B) LM cross section of wild-type flowers (arrows indicate sites of hair initiation); (C) SEM image and (D) LM cross section of *pat* flowers. Scale bars are 200 µm.

stage 1: the integument ceased development and the micropyle failed to bend downwards (Fig. 8E). Aberrant ovules were rarely distinguishable by late stage 0. At later stages, they had acquired a club shape and were intermixed with normal ovules (Fig. 8F,G), but remained smaller than these throughout the entire course of ovary development (Fig. 7B). The proportion of aberrant ovules was estimated to be 23.9±3.1% in the HRT, 55.2±8.4% in the LTR and 59.6±4.8% in the NTR environment.
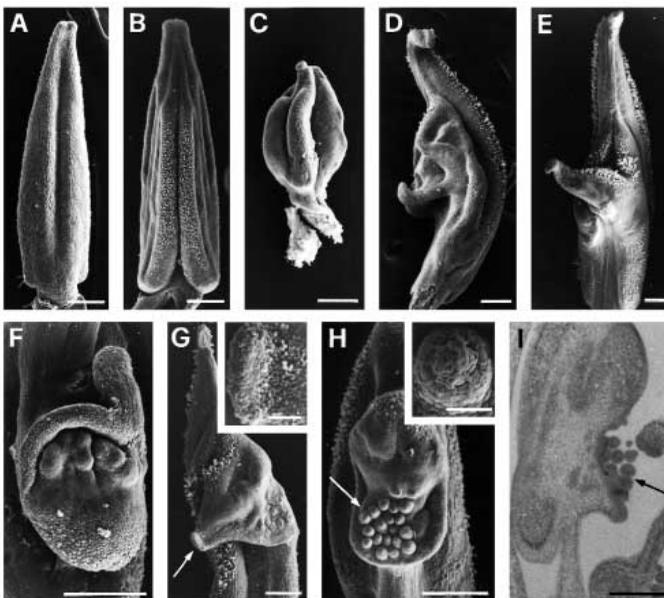

Fig. 5. Anther morphology of wild-type and *pat* flowers. (A) Abaxial and (B) adaxial SEM image of wild-type anthers, stage 0; SEM images of *pat* anthers at stages 0 (C) and 2 (D,E); detail of carpel-like structures on *pat* anthers at stage 0 (F) and 2 (G, arrow indicates stigma-like structure, detail in insert); (H) SEM and (I) LM images of a carpel-like structure bearing external ovules (arrows and insert) on a *pat* anther, stage 0. Scale bars, 250 µm (main panels); 50 µm (G insert); 25 µm (H insert).
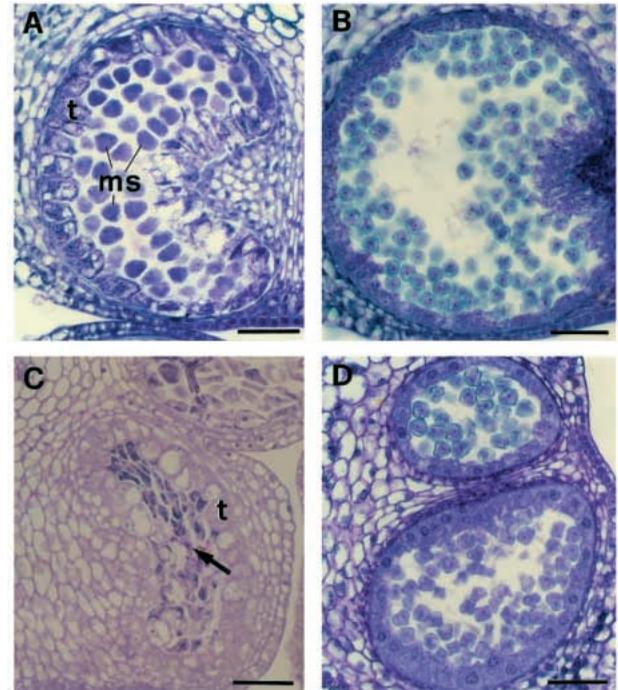

Fig. 6. LM images of microsporogenesis in wild-type and *pat* anthers. Locules of wild-type anthers showing pollen grains (A) before (stage 0) and (B) after (stage 1) tetrad release; (C) hypertrophy of the tapetum and degeneration of sporogenous tissue (arrow) in a *pat* anther at stage 0; (D) partially normal microsporogenesis in a *pat* anther at stage 1. ms, microspores, t, tapetum. Scale bars, 50 µm.

The proportion was strictly and negatively correlated with the mean number of seeds per fruit reported in Table 1. At anthesis, the placenta supporting ovules appeared as a mass of tightly compressed cells in the WT (Fig. 8H) and of looser and elongating cells in ovaries of *pat* plants (Fig. 8G,I).

Embryology of wild-type and *pat* ovaries

The archesporial cell of WT ovules was differentiated in the tenuinucellate position by stage 0 (Fig. 9A). Between stage 0 and 1, when male meiosis had already taken place and tetrads of microspores had formed, the archesporial cell enlarged and acquired the function of a megasporocyte (Fig. 9B). Female meiosis occurred during stage 1, when the germinal lineage was already protected by the integument, which had reached the level of the ovule apex (Fig. 9B,C). Megagametogenesis proceeded during stages 2 and 3 and at anthesis a mature 7-celled *Polygonum* type embryo sac was formed; at which time the nucellus had degenerated and the embryo sac had dug in 8-10 integumental cell layers. By stage 5, pollen tubes were seen to be growing on the placenta surface (data not shown).

In aberrant *pat* ovules, a megasporocyte differentiated by stage 0 (Fig. 9D), meiosis started and callose deposition occurred during stage 1 (Fig. 9E), but meiotic products and/or the formation of a normal embryo sac were never seen at later stages. Callose also frequently accumulated on the hypostatic region (Fig. 9F). At anthesis, aberrant ovules were club-shaped (Fig. 10A), open at the top and surrounded by a disorganised cellular mass (Fig. 10B,C). Occasionally, in addition to the normal and
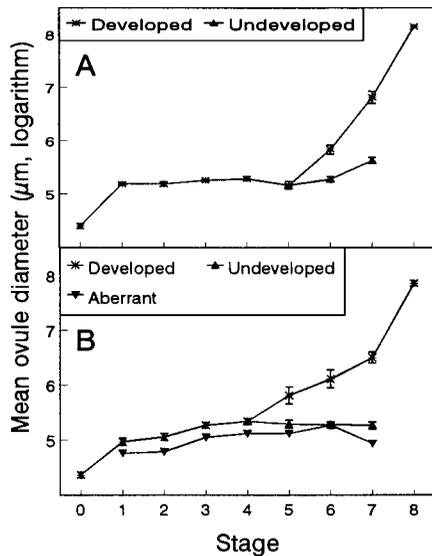
Fig. 7. Growth dynamics of developed (-✱-), undeveloped (-▲-) and aberrant (-▼-) ovules. Mean ovule diameter in (A) wild-type and (B) *pat* ovaries. Error bars represent s.e.m.

aberrant ovules, there were 'hybrid' structures which had a normally developed region and a region with an irregular mass of undifferentiated cells (Fig. 10D,E). The majority of normal, but undeveloped, ovules were unfertilised at stage 5, displayed intact synergids and polar nuclei and, by stage 6, contained a mass of relatively undifferentiated cells, highly vacuolated and bigger than the surrounding integument cells (Fig. 10F). This picture was typical of both WT and *pat* undeveloped ovules. By stage 7, most WT, but very few normal *pat* ovules were differentiating into normal seeds, containing a globular embryo, the endosperm, the endothelium and a well-developed integument (Fig. 10G).

DISCUSSION

Ovary growth is triggered before anthesis in *pat* mutants

Although the temperature regimes tested in the experiments were permissive for seed production in WT tomatoes, the degree of parthenocarpy was high and stable in *pat* mutants. In this respect, *pat* differs from other sources of parthenocarpy, such as *pat-2* (Lin et al., 1983b) and Oregon T5-4 (Bagget and Frazier, 1978), where expression is strictly temperature dependent.

Ovary development in WT tomatoes is triggered only after stage 5 (2 days post anthesis), when a mature embryo sac has been formed, pollination has occurred and fertilisation has taken place (Rick, 1980). Stage 5 marks the synchronous beginning of pericarp cell division, placenta growth and ovule development. All these processes, which

ultimately concur to initiate ovary growth, are precocious in *pat* ovaries and occur at pre-anthesis stages. At stage 3, which corresponds to 1-3 days before anthesis, *pat* ovaries are in fact significantly bigger than at the previous stage or than WT ovaries at the same stage. In *pat*, the complete machinery for fruit set and development is therefore switched on before and independently from pollen shedding, pollination and fertilisation and correlates with the expression of parthenocarpy in plants carrying the *pat-2* gene (Fos and Nuez, 1996). Although parthenocarpy, therefore, seems to be functionally similar in *pat* and *pat-2* mutants, different molecular mechanisms are likely to underlie the expression of the two genes.

pat affects floral organ identity and development

Parthenocarpy does not generally interfere with other processes of generative development. No flower aberration has been described and ovule morphogenesis and gamete production is normal in the naturally parthenocarpic tomato variety Severianin (gene *pat-2*, Lin et al., 1983a) and in auxin- and gibberellin-induced parthenocarpic fruits (Ashaira et al., 1967). In contrast, *pat* is responsible for severe modifications of flower morphology. The aberrations described for male *pat* organs show similarities with those found in some male-sterile tomato mutants (*sl*, *sl-2*, *ms15*, *ms33*) which produce shrunken stamens, bearing carpel-like structures and often external ovules (Sawhney, 1994). Among them, the *stamenless-2* (*sl-2*) mutant closely resembles *pat* in its anther development, presence of ectopic structures, course of microsporogenesis and pollen production, variation in severity and environmental
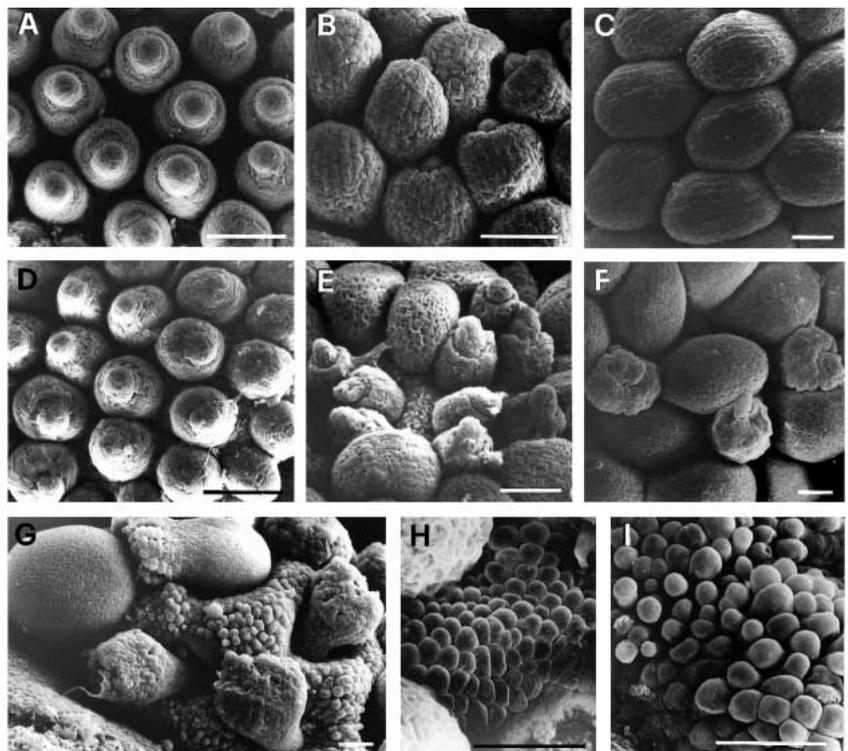

Fig. 8. SEM images of ovule and placenta development in wild-type (A-C,H) and *pat* (D-G,I) ovaries. (A) Erect ovules at stage 0; (B) bending ovules at stage 1; (C) anatropous ovules at stage 2; (D) erect *pat* ovules at stage 0; normal and aberrant *pat* ovules at stage 1 (E), 2 (F) and 5 (G); placenta cell pattern in (H) the wild type and (I) *pat* at stage 4. Scale bars are 50 μm.
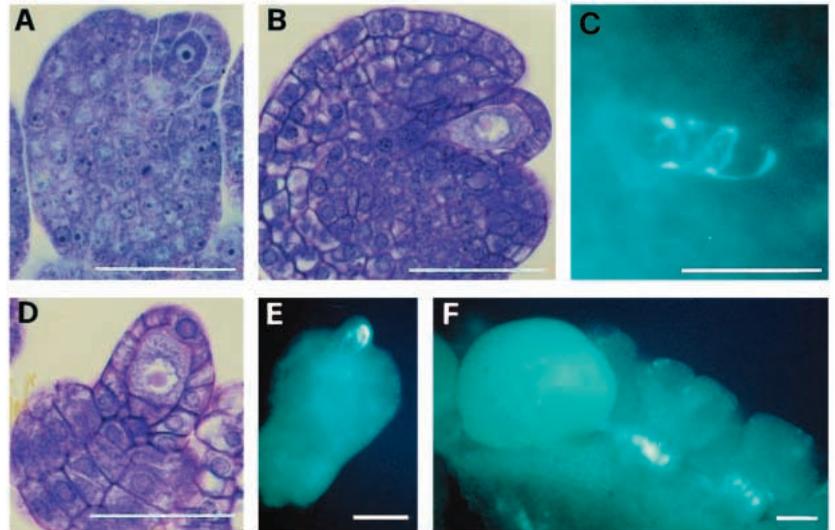
Fig. 9. Embryology of wild-type (A-C) and *pat* (D-F) ovules. (A) Archesporial cell at stage 0; (B) megasporocyte at stage 1; (C) callose deposition on a tetrad at the end of meiosis at late stage 1; (D) differentiated archesporial cell in an aberrant *pat* ovule at stage 0; (E) callose deposition on a megasporocyte and (F) on the hypostatic region of aberrant ovules at stage 1. Scale bars are 50 μm.

and hormonal sensitivity, although it exhibits no parthenocarpic tendencies (Sawhney and Greyson, 1973a).

The *pat* allele also affects ontogenetic processes during development of female reproductive organs. As expected, the production of seeds in seeded *pat* plants was very low under the growth conditions tested. We show that low seed production in *pat* is due not only to the exerted position of the stigma and anticipated ovary growth, which hamper pollination and fertilisation (Bianchi and Soressi, 1969), but also to aberrations in ovule development, which reduce the production of viable female gametes. The negative correlation between the average number of seeds per fruit (Table 1) and the proportion of aberrant ovules documented in different growth conditions indicates that ovule aberrations play a role in reducing fertility and seed set in *pat*.

Ovule development, the course of female sporogenesis and gametogenesis and the pattern of seed formation described here for WT tomato flowers support earlier embryological descriptions in this species (Cooper, 1931; Rick, 1946; Lin et al., 1983a; Nester and Zeevaart, 1988). To the best of our knowledge, *pat* is the first defective ovule mutant described in tomato; it seems to be dependent on, or connected with, disruption of the normal integument growth. Most of the ovule mutants recently described in *Arabidopsis*, *Petunia* and *Antirrhinum* (review by Angenent and Colombo, 1996) appear, from initial morphological evidence, to also involve disruptions of the integuments. All these mutants share phenotypic similarity with *pat* with respect to the reduced female fertility and the pleiotropic control exerted on different vegetative and reproductive processes. The *Arabidopsis* mutant *short integuments* (*sin1*) is in many respects the most similar to *pat*: *sin1* homozygous plants arrest the growth of ovule integuments which fail to cover the nucellus; a meiocyte is differentiated and meiosis starts, but development never

progresses beyond the tetrad stage (Robinson-Beers et al., 1992). Nevertheless, none of the genes described in the literature has to date associated alterations in ovule and flower development with parthenocarpy.

PAT has a complex regulatory function in reproductive development

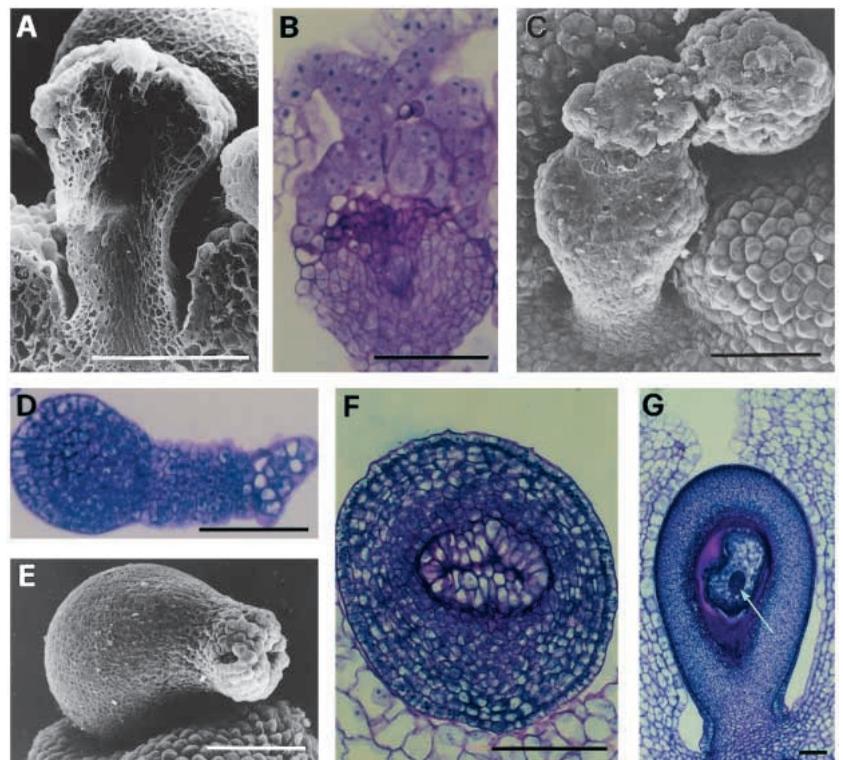The temporal succession of abnormalities in the generative

Fig. 10. Embryology of wild-type (G) and *pat* (A-F) ovules. (A) SEM image of the internal structure of an aberrant *pat* ovule at stage 4; (B) cross section and (C) SEM image of a club-shaped aberrant ovule at stage 5; (D) cross section and (E) SEM image of 'hybrid' aberrant ovules at stage 5; (F) cross section of a normal, unfertilised *pat* ovule at stage 6; (G) cross section of a fertilised wild-type ovule at stage 7 (arrow indicates the embryo). Scale bars are 100 μm.

development of *pat* plants suggests that parthenocarpy could be an induced, secondary effect of a mutated gene, whose primary function is to regulate floral organ development. Anther aberrancy, and particularly the occurrence of adaxial carpel-like structures bearing external ovules, seem to indicate that *pat* is a mutation of a putative gene with homeotic functions. Homeotic genes belonging to the family of MADS-box transcriptional factors, have recently been cloned in tomato (Pnueli et al., 1991). Antisense down-regulation of one of them, the *TM8* MADS-box gene, caused, besides deformation of the pistil and complete male and female sterility, an extremely high incidence of parthenocarpy, which occurred before the opening of the flower (Lifschitz et al., 1993). This indicates that mutations in genes expressed early to drive organ development and identity, may affect later processes, such as autonomous ovary development.

Considering that different *pat* organs are apparently defective in cell elongation, which results in short anthers, underdeveloped ovule integument and smaller sized seeds and fruits, it is intriguing to suppose that *PAT* functions interact with the GA metabolic pathway. GA_3 applications were in fact effective in reverting the *pat* anther phenotype to WT, although the same treatment was not successful in restoring female fertility (Mapelli et al., 1979). In tomato, applications of GAs also reverted flower morphology and fertility to WT levels in the male sterile *sl-2* (Sawhney and Greyson, 1973b) and in completely sterile gibberellin-deficient mutants (Nester and Zeevaart, 1988). Studies that included histological details were not carried out in either case. However, the mechanisms underlying the altered function of *pat* are not likely to be clarified until the gene is cloned and fully characterized. Research in this direction is in progress.

All the characteristics of *pat* expression we have described make this mutation of prime interest for clarifying the complex interactions that take place between the genetic, hormonal and environmental control of flower ontogenesis and fruit set. Because tomato is not simply an important vegetable crop, but also an experimental tool favoured by geneticists and now even molecular biologists, it is foreseeable that the body of knowledge on flower development garnered in model species will be transferred to experimental systems of *Lycopersicon*, where genetics is much advanced and a large number of flower mutants is available.

REFERENCES

Angenent, G. and Colombo, L. (1996). Molecular control of ovule development. *Trends Plant Sci.* **1**, 228-232.

Ashaira, T., Takeda, Y., Nishio, T., Hirabayashi, M. and Tsukamoto, Y. (1967). Studies on fruit development in tomato. I. Ovule development and content of diffusible auxin in synthetic auxin- and gibberellin-induced parthenocarpic tomato fruits in relation to their development. *Mem. Res. Inst. Food Sci., Kyoto Univ.* **28**, 47-74.

Bagget, J. R. and Frazier, W. A. (1978). Oregon T5-4 parthenocarpic tomato line. *HortSci.* **13**, 599.

Bianchi, A. and Soressi, G. P. (1969). Mutanti di pomodoro artificialmente indotti suscettibili di utilizzazione nel miglioramento genetico. *Sementi Elette* XV (3), 2-6.

Cooper, D. C. (1931). Macrosporogenesis and the development of the macrogametophyte of *Lycopersicon esculentum. Amer. J. Bot.* **18**, 739-748.

Falavigna, A. and Soressi, G. P. (1987). Influence of the *pat-sha* gene on plant and fruit traits in tomato (*L. esculentum* Mill.). In *Modern Trends in Tomato Genetics and Breeding*. p. 128. Proceedings of the 10th Meeting of the EUCARPIA Tomato Working Group, 2-6 Sept. 1987, Salerno, Italy.

Falavigna, A., Badino, M. and Soressi, G. P. (1978). Potential of the monomendelian factor *pat* in the tomato breeding for industry. *Genetica Agraria* **32**, 159-160 (Abstr.).

Fos, M. and Nuez, F. (1996). Molecular expression of genes involved in parthenocarpic fruit set in tomato. *Physiol. Plant.* **98**, 165-171.

George, W. L., Scott, J. W. and Splittstoesser, W. E. (1984). Parthenocarpy in tomato. *Hort. Rev.* **6**, 65-84.

Gillaspy, G., Ben-David, H. and Gruissem, W. (1993). Fruits: A developmental perspective. *Plant Cell* **5**, 1439-1451.

Gustafson, F. G. (1936). Inducement of fruit development by growth-promoting chemicals. *Proc. Natl. Acad. Sci. U.S.A.* **22**, 628-636.

Lifschitz, E., Brodai, L., Hareven, D., Hurwitz, C., Prihadash, A., Pnueli, L., Samach, A. and Zamir, D. (1993). Molecular mapping of flower development in tomato. In *Molecular Biology of Tomato* (ed. J. Yoder), pp. 175-184. Technomic Publishing Co. Inc., Lancaster PA, USA.

Lin, S., Splittstoesser, W. E. and George, W. L. (1983a). A comparison of normal seeds and pseudoembryos produced in parthenocarpic fruits of 'Severianin' tomato. *HortSci.* **18**, 75-76.

Lin, S., Splittstoesser, W. E. and George, W. L. (1983b). Factors controlling the expression of parthenocarpy in 'Severianin' tomato. *Sci. Hort.* **19**, 45-53.

Mapelli, S., Frova, C., Torti, G. and Soressi, G. P. (1978). Relationship between set, development and activities of growth regulators in tomato fruits. *Plant Cell Physiol.* **19**, 1281-1288.

Mapelli, S., Torti, G., Badino, M. and Soressi, G. P. (1979). Effects of GA_3 on flowering and fruit-set in a mutant of tomato. *HortSci.* **14**, 736-737.

McIntosh, M. S. (1983). Analysis of combined experiments. *Agron. J.* **75**, 153-155.

Nester, J. E. and Zeevaart, J. A. D. (1988). Flower development in normal tomato and a gibberellin-deficient (*ga-2*) mutant. *Amer. J. Bot.* **75**, 45-55.

Nitsch, J. P. (1970). Hormonal factors in growth and development. In *Food Science and Technology* (ed. A.C. Hulme), vol. 1, pp. 427-472. Academic Press, London.

Pecaut, P. and Philouze, J. (1978). A *sha pat* line obtained by natural mutation. *Rep. Tom. Genet. Coop.* **28**, 12.

Philouze, J. (1983). Parthénocarpie naturelle chez la tomate. I. – Revue bibliographique. *Agronomie* **3**, 611-620.

Philouze, J. (1985). Parthénocarpie naturelle chez la tomate. II. – Etude d'une collection variétale. *Agronomie* **5**, 47-54.

Philouze, J. and Pecaut, P. (1986). Parthénocarpie naturelle chez la tomate. III. – Etude de la parthénocarpie due au gène *pat* (*parthenocarpic fruit*) de la lignée 'Montfavet 191'. *Agronomie* **6**, 243-248.

Pnueli, L., Abu-Abeid, M., Zamir, D., Nacken, W., Schwarz-Sommer, Sh. and Lifschitz, E. (1991). The MADS box gene family in tomato: temporal expression during floral development, conserved secondary structures and homology with homeotic genes from *Antirrhinum* and *Arabidopsis*. *Plant J.* **1**, 255-266.

Rick, C. M. (1946). The development of sterile ovules in *Lycopersicon esculentum* Mill. *Amer. J. Bot.* **33**, 250-256.

Rick, C. M. (1980). Tomato. In *Hybridization of Crop Plants* (ed. W. R. Fehr and H. H. Hadley), pp. 669-680. American Society of Agronomy, Madison, USA.

Robinson-Beers, K., Pruitt, R. E. and Gasser, C. S. (1992). Ovule development in wild-type *Arabidopsis* and two female sterile mutants. *Plant Cell* **4**, 1237-1249.

Sawhney V. K. 1994. Genic male sterility in tomato and its manipulation in breeding. In *Genetic Control of Self-Incompatibility and Reproductive Development in Flowering Plants* (ed. E. G. Williams, A. E. Clarke and R. B. Knox), pp. 443-458. Kluwer Acad. Publ., Dordrecht, The Netherlands.

Sawhney, V. K. and Greyson, R. I. (1973a). Morphogenesis of the *stamenless-2* mutant in tomato. I. Comparative description of the flowers and ontogeny of stamens in the normal and mutant plants. *Amer. J. Bot.* **60**, 514-523.

Sawhney, V. K. and Greyson, R. I. (1973b). Morphogenesis of the *stamenless-2* mutant in tomato. II. Modifications of sex organs in the mutant and normal flowers by plant hormones. *Can. J. Bot.* **51**, 2473-2479.

Soressi, G. P. and Salamini, F. (1975). A monomendelian gene inducing parthenocarpic fruits. *Rep. Tom. Genet. Coop.* **25**, 22.